Polymer 50 (2009) 1223–1227

Contents lists available at ScienceDirect

Polymer

journal homepage: www.elsevier.com/locate/polymer

Oxidation effect on templating of metal oxide nanoparticles within block copolymers

Pinar Akcora [a,1], Robert M. Briber [b], Peter Kofinas [c,*]

[a] Department of Chemical and Biomolecular Engineering, University of Maryland, College Park, MD, United States
[b] Department of Materials Science and Engineering, University of Maryland, College Park, MD, United States
[c] Fischell Department of Bioengineering, University of Maryland, Bldg 225 Room 1120, College Park, MD 20742-2111, United States

ARTICLE INFO

Article history:
Received 20 August 2008
Received in revised form
29 December 2008
Accepted 10 January 2009
Available online 15 January 2009

Keywords:
Block copolymer
Nanoparticle
Templating

ABSTRACT

Amphiphilic norbornene-*b*-(norbornene dicarboxylic acid) diblock copolymers with different block ratios were prepared as templates for the incorporation of iron ions using an ion exchange protocol. The disordered arrangement of iron oxide particles within these copolymers was attributed to the oxidation of the iron ions and the strong interactions between iron oxide nanoparticles, particularly at high iron ion concentrations, which was found to affect the self-assembly of the block copolymer morphologies.

1. Introduction

Organic–organometallic block copolymers [1–3], functionalized copolymers with tailored interactions [4–8], and block copolymer micelles [9–13] have been utilized as templates to produce ordered inorganic nanoparticle arrays. Ring-opening metathesis polymerization has been used to polymerize charged metal complexes [14–16] and charged monomers [17]. An alternative route of coordinating metal ions in a specific block of a copolymer is mixing polymers with metal salts in a common solvent. Amphiphilic block copolymers such as poly(styrene-*b*-acrylic acid) (PS-PAA) and poly(norbornene-*b*-norbornene dicarboxylic acid) (NOR-NORCOOH) have been synthesized and processed to template metal oxide nanoparticle arrays within the self-assembled copolymer morphologies [18]. The carboxylic acid groups in the PAA and NORCOOH blocks allow for the selective loading of iron ions, which is followed by oxidation of iron ions into iron oxide particles. In our previous work, the dispersion of iron oxide nanoparticles was examined by transmission electron microscopy within various norbornene/norbornene dicarboxylic acid copolymers with different block compositions [19]. Small-angle neutron scattering experiments on iron oxide doped and undoped copolymers showed that the diblock copolymer morphology was distorted by the presence of the nanoparticles [19]. We have studied the effect of different doping methods on particle self-assembly, to understand the various factors influencing the microphase separation of copolymers with nanoparticles. When thin films (thickness of ~50 nm) of pure copolymers were immersed in an iron salt solution, iron ions were more likely associated with the carboxylic acid containing block of the copolymer, and arrays of particles were formed within block copolymer templates. These results suggest that spherical iron oxide nanoparticles can be templated at low particle density within thin films (~50 nm thickness) after oxidation [20].

Control on size and spatial dispersion can result in nanoparticles with quantum-size effects. Block copolymers with iron oxide nanoparticles have been used, for example, in the development of nanocomposites with enhanced magnetic and dielectric properties at radio frequencies [21]. Here, we show that the oxidation step becomes critical in the organization of iron oxide nanoparticles within the bulk block copolymer films. We have examined the iron ion dispersion within the poly(norbornene-*b*-norbornene dicarboxylic acid) copolymer films before and after oxidizing the metal ions into metal oxides. The carboxylic acid containing block of the norbornene copolymer has been used to uptake the iron ions, and the uncoordinated metal ions were subsequently washed out with water. We have characterized the (undoped) norbornene based diblock copolymer morphologies of bulk films and the dispersion of iron oxide particles within these copolymer templates using transmission electron microscopy (TEM) and small-angle X-ray scattering (SAXS).

* Corresponding author. Tel.: +1 301 405 7335; fax: +1 301 405 0523.
E-mail address: kofinas@umd.edu (P. Kofinas).
[1] Current address: University of Missouri, Department of Chemical Engineering, Columbia, MO 65211, United States.

0032-3861/$ – see front matter © 2009 Elsevier Ltd. All rights reserved.
doi:10.1016/j.polymer.2009.01.020

Table 1
Copolymer compositions, observed morphologies and iron ion (Fe^{+3}) amounts before/after NaOH washing for the NOR/NORCOOH copolymer nanocomposites used in this work.

Volume fraction ($\phi_{NORCOOH}$)	Morphology	Fe (wt%) before washing	Fe (wt%) after washing
0.2	Spherical	4	4
0.36/0.5	Cylindrical	7.4/9.4	6/7
0.6	Lamellar	11.7	10

2. Experimental

Norbornene-deuterated norbornene dicarboxylic acid diblock copolymers (NOR/d-NORCOOH) with 0.2, 0.36, 0.50 and 0.60 volume fractions of d-NORCOOH were synthesized by ring-opening metathesis polymerization (ROMP) and then mixed with iron salts in solution [19]. These iron salt–polymer solutions were cast into films in a solvent saturated atmosphere in a desiccator. The films were subsequently soaked in NaOH solution and then in water to form iron oxide nanoparticles following previously reported procedures [19]. The polydispersity indices for the corresponding samples, measured using GPC/LS, were 1.46, 1.67, 1.24 and 1.23, respectively. Block copolymer morphologies and particle dispersion in the copolymer nanocomposites were examined by TEM (Hitachi H-600, operated at 100 keV). The volume fraction of the NORCOOH block, the observed undoped polymer morphologies, and calculated and actual Fe^{+3} amounts in the doped samples are given in Table 1. Iron amounts in these samples were determined from elemental analysis, indicating that samples upload most of the Fe^{+3} ions incorporated in them. Films were microtomed to ~50 nm thickness using a Leica EM UC6 microtome at room temperature with a diamond knife. The pure block copolymer morphology was examined after staining the microtomed sections with iodine vapor in a closed desiccator at room temperature for 3 h. Small-angle X-ray scattering measurements on iron doped and undoped samples were performed at beamline 12-ID (BESSRC) at the Advanced Photon Source. The dispersion of ions and iron oxide nanoparticles after complete oxidation was examined for the sample with 4 wt% iron. The SAXS data of this sample represent the ion ordering (which is partially oxidized to metal oxides in air) prior to complete oxidation with NaOH.

3. Results and discussion

Pure (undoped) block copolymer morphologies were examined by TEM after staining the samples with iodine. The extent of

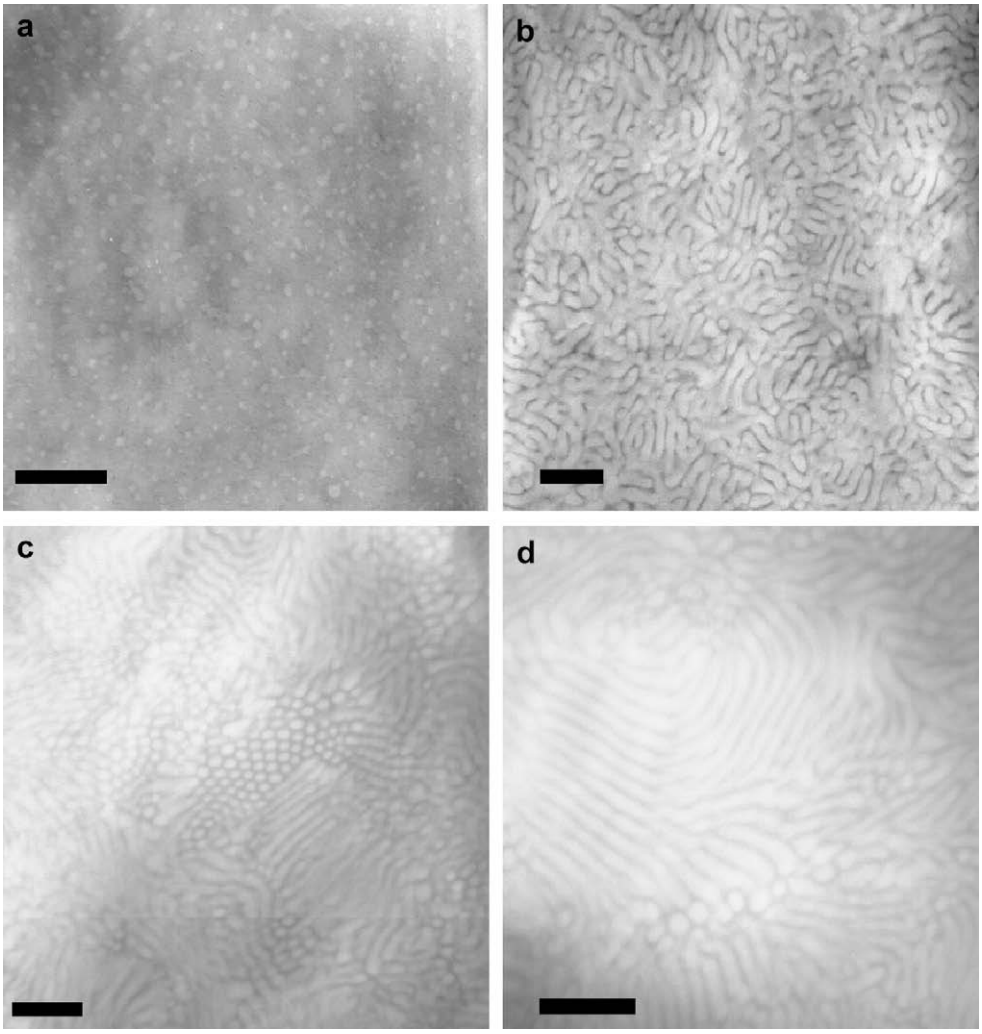

Fig. 1. Electron micrographs of NOR/d-NORCOOH diblock copolymers showing (a) spherical microphase separation, where the volume fraction of the NORCOOH block is 0.2; (b), (c) cylindrical and (d) lamellar microstructures are observed for the copolymers with 0.36, 0.5 and 0.6 volume fractions of NORCOOH block, respectively. Microstructures shown are non-equilibrium morphologies. The norbornene block is preferentially stained with iodine vapor.

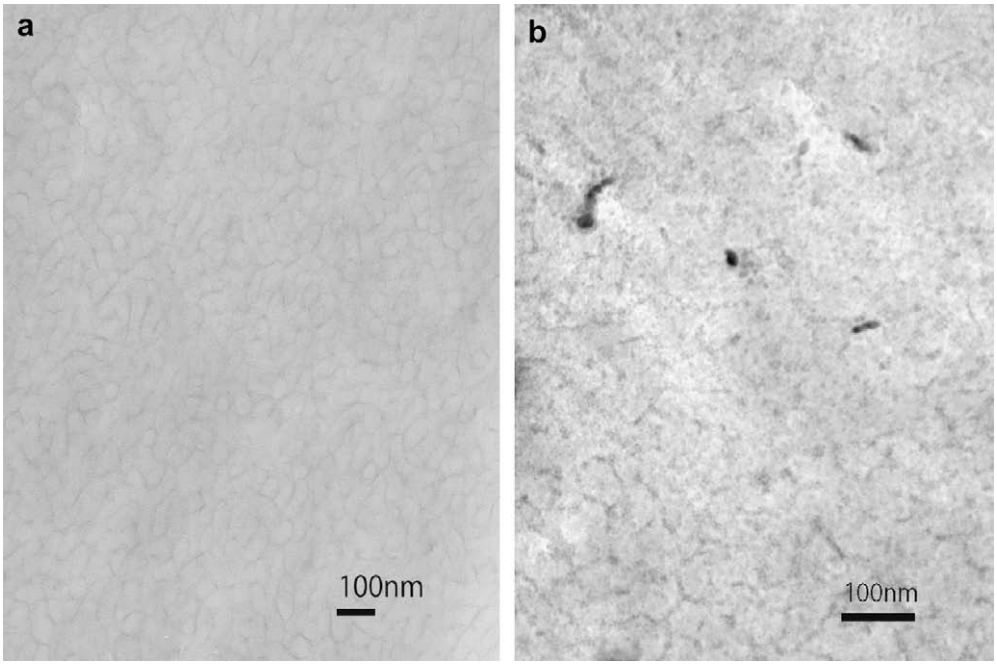

Fig. 2. Electron micrographs of Fe^{+3} doped NOR/d-NORCOOH diblock copolymer with NORCOOH volume fraction of 0.2 (a) before oxidation, (b) after oxidation to Fe_2O_3 using a NaOH solution wash.

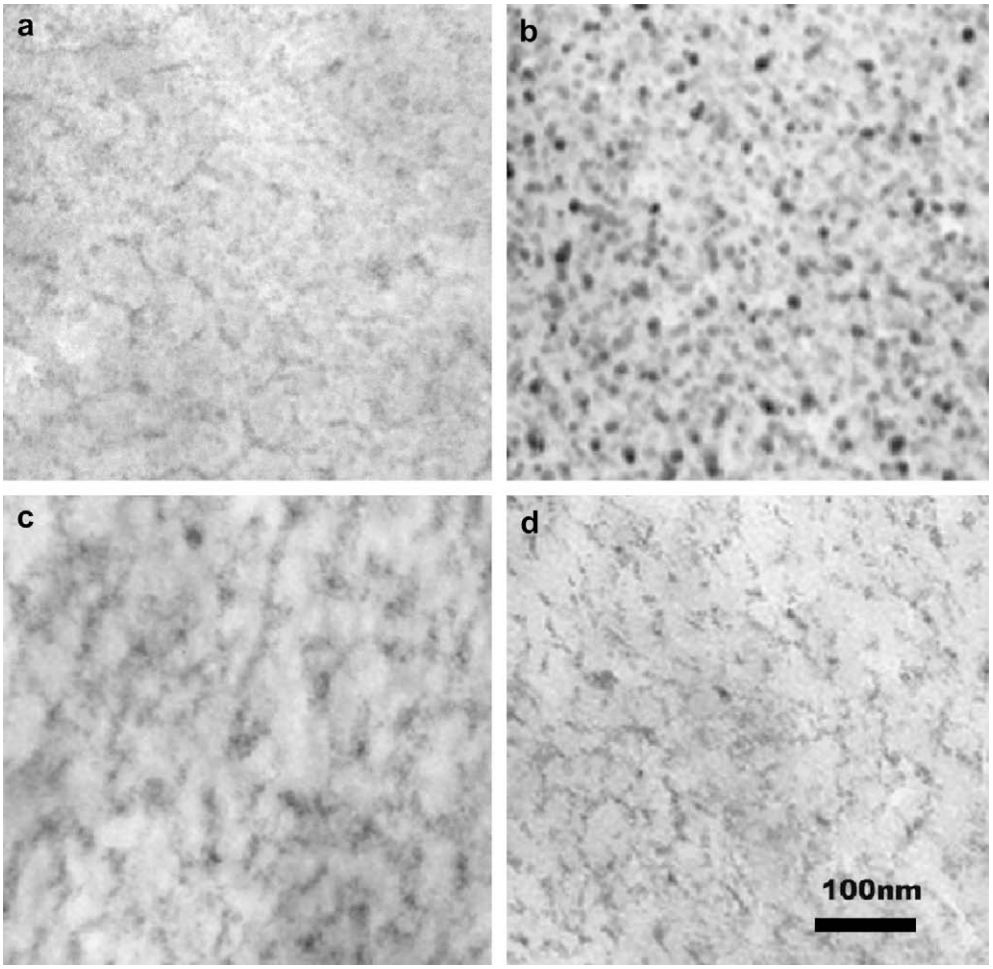

Fig. 3. Electron micrographs of Fe_2O_3 doped NOR/d-NORCOOH diblock copolymers. The volume fraction of the NORCOOH block is (a) 0.2, (b) 0.36, (c) 0.5 and (d) 0.6, respectively. Images show the dispersion of iron oxide nanoparticles in different copolymers after oxidation to Fe_2O_3 using NaOH.

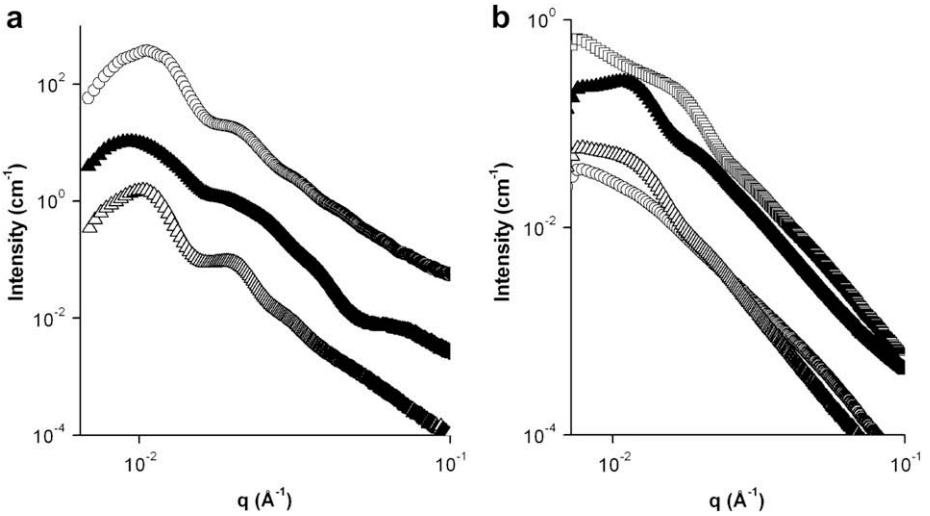

Fig. 4. SAXS profiles of (a) pure NOR/d-NORCOOH and (b) γ-Fe_2O_3 doped diblock copolymers. The volume fraction of the NORCOOH domain ($\phi_{NORCOOH}$) varies from 0.2 to 0.6. Volume fractions' ratio corresponds to that of norbornene and norbornene dicarboxylic acid blocks, respectively. Spheres are for the 0.4/0.6; open triangles are for the 0.64/0.36; filled triangles are for the 0.8/0.2 and squares are for the 0.5/0.5 which are the ratio of volume fractions for NOR/NORCOOH. Scattering from metal particles dominate the copolymer structure. Peaks in (b) refer to iron oxide particle ordering. All polymer–metal hybrid composites excluding the sample with the smallest $\phi_{NORCOOH}$: 0.2 are oxidized through a NaOH wash. Particles are better dispersed in the unoxidized sample, as represented by filled triangles ($\phi_{NOR}/\phi_{NORCOOH}$: 0.8/0.2). Templating becomes ineffective after oxidation. Curves are shifted vertically for clarity.

staining depends on the physical absorption of iodine in the norbornene block of the copolymer. TEM micrographs have shown the expected spherical, cylindrical and lamellar morphologies (Fig. 1) of the pure diblock copolymers with increasing NORCOOH block volume fraction. The sample with the smallest volume fraction of NORCOOH ($\phi_{NORCOOH}$: 0.2) block shows some ordering of the iron ions in the copolymer matrix template (Fig. 2a). The metal ions exhibit an interconnected morphology which looks like spherical shells before neutralization. These structures resemble the vesicular Cs ion aggregates within polystyrene-*ran*-methacrylic acid copolymers reported by Winey et al. [22]. We prepared the samples by microtoming the bulk film and collected the sections floating on water. We believe that the thin film was not neutralized at the sample preparation step and exhibits the interconnected morphology which is expected to be a metastable morphology of ions. A thin film (around ~100 nm thickness) of the same sample was immersed in NaOH solution for 10 min and later rinsed with water. The oxidized film displayed a slight distortion of the templated morphology and the spherical iron oxide particles were observed after the oxidation (Fig. 2b). Note that Fig. 2b shows the iron oxide nanoparticle dispersion in an oxidized thin film. Another factor that explains the interconnected aggregates of ions prior to oxidation is that the carboxylic acid containing block swells in NaOH solution, thereby allowing migration of ions which can result in the formation of the observed shell-like aggregated structures. We make the comparison of observed morphologies of ions and iron oxide particles within the one sample only.

For the samples with higher volume fractions ($\phi_{NORCOOH}$ varies from 0.36 to 0.6), a disordered particle dispersion was observed after oxidation to Fe_2O_3 as shown in Fig. 3b–d. While spherical iron oxide particles with mean size of 5 nm are observed in Fig. 3b, the non-spherical connected aggregates of particles are seen with increasing iron concentrations in Fig. 3c and d. We believe that the interconnected microstructures observed in these oxidized samples can be due to the strong interactions at higher iron ion loadings (greater than 6 wt% Fe) which were previously shown to be affecting the copolymer morphologies [19].

Next we compare the small-angle X-ray scattering profiles of undoped and iron oxide doped copolymers with varying NORCOOH volume fractions ($\phi_{NORCOOH}$) from 0.2 to 0.6. It is clear from Fig. 4a that all undoped copolymers show ordered structures with an average spacing of ~45 nm. SAXS data from the sample with $\phi_{NORCOOH} = 0.36$ and 0.5 showed higher order scattering maxima at $\sqrt{3}$ and $\sqrt{9}$ (the numbers refer to the ratio of the peak positions relative to the first order peak), most likely indicating cylindrical microphase separated domains. However, characteristic peaks for the lamellar and spherical morphologies cannot be assigned which might be due to the large PDIs of the synthesized polymers. The scattering profiles of the (doped) samples (Fig. 4b) – with the exception of sample containing 4 wt% Fe – show poor ordering of the iron oxide particles. The sample containing 4 wt% Fe (NORCOOH volume fraction of 0.2) shows a clear peak indicating that iron ions exhibit strong ordering before oxidation, which is consistent with the interconnected structures seen in Fig. 2a. Our SAXS results coupled with observations by TEM indicate that the nanoparticles form distorted interconnected structures after oxidation to iron oxides. The observed morphologies therefore strongly depend on particle concentration and oxidation time, which varies for the thin film and melts.

The process of ion exchange is based on the coordination of Fe^{+3} to the $-COO^{-1}$ group on the block copolymer chain, while the Cl^{-1} ion coordinates to the proton of the carboxylic acid due to the strong acid bond formation. During the NaOH wash treatment, sodium carboxylates become carboxylic acid groups, and the iron hydroxyls are quickly transformed to iron oxide nanoparticles [23]. The interaction between iron ions during this solution doping process, and the possible changes in polymer chain conformation at high ion loadings can affect the copolymer self-assembly and metal oxide nanoparticle dispersion in the solid state. Simulations of Balazs et al. have shown that the strength of interaction between polymer domains and nanoparticles can alter the copolymer morphology [24–26]. SANS results shown in our previous work confirm that the block copolymer morphology can be distorted at high particle loadings [19]. A similar effect of metal concentration on the morphology of (PS-PVP) block copolymer/Au nanocomposites has been observed by Lo et al. [27]. It has also been shown that by increasing the iron oxide nanoparticle

concentration, the morphology of the (PS-PI) block copolymers becomes more disordered, losing long range correlations [28].

4. Conclusion

Neutralization of the associated iron ions within the block copolymer changes the dispersion of the resultant iron oxide nanoparticles in block copolymer melts. Spherical shell-like aggregates of Fe^{+3} ions at 4 wt% were formed into disordered interconnected iron oxide aggregates after oxidation. While spherical iron oxide nanoclusters are observed at 6 wt% Fe, interconnected and non-spherical morphologies of iron oxide particles were seen with increasing iron content. Our results suggest that oxidation is one of the factors controlling the dispersion of the iron oxide particles within the copolymer templates. Other factors such as magnetic dipolar interactions can lead to disordered iron oxide particles after oxidation.

Acknowledgements

This material is based upon work supported by the Air Force Office of Scientific Research, Grant # FA95500610097. Use of the Advanced Photon Source at Argonne National Laboratory was supported by the U.S. Department of Energy, Office of Science, Office of Basic Energy Sciences, under Contract No. DE-AC02-06CH11357. We thank Dr. Soenke Seifert for small-angle X-ray scattering measurements.

References

[1] Cheng JY, Ross CA, Chan VZH, Thomas EL, Lammertink RGB, Vancso GJ. Adv Mater 2001;13:1174.
[2] Eitouni HB, Balsara NP. J Am Chem Soc 2004;126:7446.
[3] Thurn-Albrecht T, Schotter J, Kastle GA, Emley N, Shibauchi T, Krusin-Elbaum L, et al. Science 2000;290:2126.
[4] Lin Y, Boker A, He J, Sill K, Xiang H, Abetz C, et al. Nature 2005;434:55.
[5] Shan J, Tenhu H. Chem Commun 2007;44:4580.
[6] Sohn BH, Seo BH. Chem Mater 2001;13:1752.
[7] Thompson RB, Ginzburg VV, Matsen MW, Balazs AC. Science 2001;292:2469.
[8] Belfield KD, Zhang L. Chem Mater 2006;18:5929.
[9] Bennett RD, Xiong GY, Ren ZF, Cohen RE. Chem Mater 2004;16:5589.
[10] Koh H-D, Kang N-G, Lee J-S. Langmuir 2007;23:11425.
[11] Stubenrauch K, Moitzi C, Fritz G, Glatter O, Trimmel G, Stelzer F. Macromolecules 2006;39:5865.
[12] Smith D, Pentzer EB, Nguyen ST. Polym Rev 2007;47:419.
[13] Mandal D, Chatterjee U. J Chem Phys 2007;126:134507.
[14] Abd-El-Aziz AS, May LJ, Hurd JA, Okasha RM. J Polym Sci Part A Polym Chem 2001;39:2716.
[15] Stanton CE, Lee TR, Grubbs RH, Lewis NS. Macromolecules 1995;28:8713.
[16] Gibbs JM, Park S, Anderson DR, Watson KJ, Mirkin CA, Nguyen ST. J Am Chem Soc 2005;127:1170.
[17] Nair KP, Weck M. Macromolecules 2007;40:211.
[18] Zhang MF, Estournes C, Bietsch W, Muller AHE. Adv Funct Mater 2004;14:871.
[19] Akcora P, Zhang X, Varughese B, Briber RM, Kofinas P. Polymer 2005;46:5194.
[20] Akcora P, Briber RM, Kofinas P. Polymer 2006;47:2018.
[21] Yang T-I, Brown RN, Kempel LC, Kofinas P. J Magn Magn Mater 2008;320:2714.
[22] Kirkmeyer BP, Taubert A, Kim J-S, Winey KI. Macromolecules 2002;35:2648.
[23] Ahmed SR, Kofinas P. Macromolecules 2002;35:3338.
[24] Balazs AC. Curr Opin Colloid Interface Sci 2000;4:443.
[25] Balazs AC, Ginzburg VV, Qiu F, Peng G, Jasnow D. J Phys Chem 2000;104:34.
[26] Huh J, Ginzburg VV, Balazs AC. Macromolecules 2000;33:8085.
[27] Lo C-T, Lee B, Pol VG, Rago NLD, Seifert S, Winans RE, et al. Macromolecules 2007;40:8302.
[28] Park MJ, Park J, Hyeon T, Char K. J Polym Sci Part B Polym Phys 2006;44:3571.